Experimental Spin Density in a Purely Organic Free Radical: Visualisation of the Ferromagnetic Exchange Pathway in *p*-(Methylthio)phenyl Nitronyl Nitroxide, Nit(SMe)Ph

Yves Pontillon,[b, c] Andrea Caneschi,[a] Dante Gatteschi,*[a] Andre Grand,[b] Eric Ressouche,[b] Roberta Sessoli,[a] and Jacques Schweizer*[b]

Abstract: The $P2_1/a$ form of the 2-(4-methylthiophenyl)-4,4,5,5-tetramethylimidazoline-1-oxyl-3-oxide [Nit(SMe)Ph] ferromagnet ($T_c = 0.2$ K) was investigated by conventional and polarised neutron diffraction. The data was analysed by both direct methods (3D maximum entropy) and indirect methods (wave function modelling). In both cases, we found that the major part of the spin density is located on the O-N-C-N-O fragment with a negative contribution on the bridging sp^2 carbon atom. In addition, the magnetic molecular orbital of the two oxygen atoms of the O-N-C-N-O fragment is rotated and hybridised. Delocalisation of the unpaired electron onto the methylthio fragment is significant; it suggests that this group is involved in the intermolecular exchange pathway. The experimental results were compared to those obtained by density functional theory (DFT) calculations on an isolated molecule as well as on a pair of molecules which have the same short intermolecular contact as those observed in the structure. The main conclusion is that DFT fails to predict, in terms of quantitative results, the transfer and the delocalisation of the spin density outside of the O-N-C-N-O fragment.

Keywords: density functional calculations · electron transfer · magnetic properties · neutron diffraction · radicals · spin density

Introduction

Molecular magnetism is a rapidly developing field that combines the skills of experimental and theoretical scientists. The spin-labelling technique[1, 2] strongly contributed to the development of the organic chemistry of nitroxide free radicals.[3, 4] Since the reported synthesis[5] of stable 2-phenyl-4,4,5,5-tetramethylimidazoline-1-oxyl-3-oxide, NitPh, considerable effort has been devoted to the physical characterisation of Ullman's nitronyl nitroxide free radicals **A**.

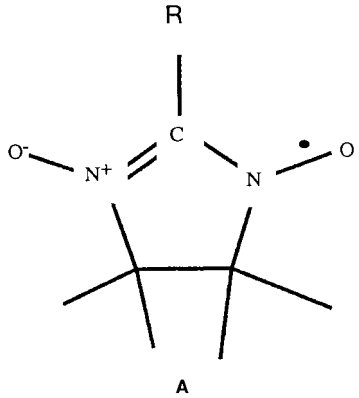

A

These compounds carry a delocalised, $S = 1/2$, unpaired electron. Some of their derivatives were found to be paramagnetic at low temperature (NitPh[5]), while others were found to exhibit cooperative magnetic behaviour.[6–11] In particular, Nit(pNO$_2$)Ph was found to be the first genuine organic ferromagnet.[12] This magnetic behaviour is very sensitive to the chemical structure of the spin carrier and to the crystal packing. In fact, Nit(pNO$_2$)Ph crystallises in four different phases, of which only the β phase orders ferromagnetically ($T_c = 0.6$ K).[13, 14] Moreover, the attachment of the nitro group in the *meta*-, rather than in the *para*- position of the phenyl, leads to an antiferromagnetic compound.[6] This early discovery precipitated a number of investigations of many other Nit radicals and a few of them were found to order ferromagnetically with T_c values in the range 0.2 – 0.6 K.[15] In

[a] Prof. D. Gatteschi, A. Caneschi, R. Sessoli
Dipartimento di Chimica, Università degli Studi di Firenze, Via Maragliano 77, I-50144 Florence (Italy)
Fax: (+39) 55-35-48-45
E-mail: gattesch@blu.chim1.unifi.it

[b] Dr. J. Schweizer, Y. Pontillon, A. Grand, E. Ressouche
Commissariat à l'Energie Atomique, MDN/SPSMS/DRFMC, CEN-Grenoble
17 rue des Martyrs, F-38054 Grenoble Cedex 9 (France)
Fax: (+33) 4-76-88-51-09
E-mail: jacques.schweizer@cea.fr

[c] Present address:
Università degli Studi di Firenze (Italy)

  0947-6539/99/0512-3616 $ 17.50+.50/0

the meantime, a nitroxide radical was found to order ferromagnetically at 1.48 K.[16] Several possible mechanisms leading to ferromagnetic coupling between the nitronyl nitroxide radicals were suggested; however, experimental evidence has been controversial, and statistical elaborations have so far been unsuccessful in providing unequivocal evidence on the most efficient pathways which lead to ferromagnetic coupling.[17] The problem is that the interactions are weak in all cases, and a detailed knowledge of the unpaired spin-density map should be obtained experimentally and then associated with theoretical calculations in order to substantiate qualitative conclusions.

Neutrons, thanks to their magnetic moment, are a unique tool for spin-density studies.[18] On the one hand they can be used to measure microscopic distributions of spin densities as opposed, for example, to macroscopic measurements, such as the magnetic susceptibility. On the other hand, unlike the resonance techniques which measure microscopic quantities at certain points of the molecule, neutrons are itinerant probes which provide information on the spin density at every point in the crystal.

Neutrons are scattered by nuclear interactions with the nuclei and by magnetic interactions with the spin density. Under the experimental conditions, the nuclear spins are not polarised and the nuclear scattering is independent of the neutron spin. In contrast, the electronic spins are polarised by a magnetic field and the interaction of the neutron with the spin density depends on the neutron spin. This allows the separation of the magnetic and the nuclear contributions by the use of a polarised neutron beam and different beam polarisations.

Polarised neutron diffraction studies of a paramagnetic single crystal are usually performed by inducing a magnetisation density by means of a strong magnetic field at low temperature. The induced magnetisation density is periodic as is the nuclear density. For this reason, all the coherent elastic scattering occurs at the Bragg positions (*hkl*).

In practice one measures the so-called "flipping ratio" R of Bragg reflections, that is the ratio of scattered intensities for "up" (parallel to the applied field) and "down" (antiparallel) polarisations of the incident beam. Moreover, if the crystal structure is centrosymmetric, the expression for R is given by Equation (1) $[\vec{F}_M = \vec{z}F_M;\quad F_{M\perp} = F_M\sin\alpha;\quad F_{M\perp z} = F_M\sin^2\alpha]$, where α is the angle between the scattering vector (*hkl*) and $\vec{z}$, where $\vec{z}$ is a unit vector along the applied magnetic field, F_N is the nuclear structure factor and $\vec{F}_M$ is the magnetic structure factor (Fourier component of the magnetisation density).

$$R_{(h,k,l)} = \frac{I\uparrow}{I\downarrow} = \frac{F_N^2 + F_{M_\perp}^2 + 2F_N F_{M_{\perp z}}}{F_N^2 + F_{M_\perp}^2 - 2F_N^2 F_{M_{\perp z}}^2} \qquad (1)$$

If the crystal structure is known, the F_N values are known and the magnetic structure factors can be extracted from Equation (1). Consequently, the experiment generally includes two steps. In the first one, conventional unpolarised neutron diffraction techniques are used to determine the precise structure of the crystal at low temperature, including the location of the hydrogen atoms and the thermal parameters. In the second step the flipping ratios are measured with polarised neutrons at low temperature to maximise the amount of ordered spin density induced by the applied field.

We report herein a single-crystal polarised-neutron investigation and ab initio calculations of the spin density of a purely organic nitronyl nitroxide free radical which exhibits ferromagnetic ordering: the 2-(4-methylthiophenyl)-4,4,5,5-tetramethylimidazoline-1-oxyl-3-oxide, Nit(SMe)Ph (T_c = 0.2 K[19]). The magnetic interactions observed in this compound were attributed to an exchange pathway which involves the NO group of one molecule and the SMe group of a neighbouring molecule, on the basis of spin-diffusion effects observed in EPR spectroscopy. In particular, it was assumed that the S atom, with its expanded electron cloud could play a major role. We show herein how the polarised neutron data modify this view and how they suggest a definite mechanism for the magnetic interaction. Furthermore, we compare the distribution of the spin density in Nit(SMe)Ph with that of a related compound, the phenyl-substituted nitronyl nitroxide NitPh,[20] in which the molecules are isolated with practically no intermolecular magnetic interaction. Thus, we can compare the results obtained for the two related species and derive important magneto-structural correlations by consideration of the role played by the crystal packing and by the methylthio group in the redistribution of the spin density within the radical and, consequently, in the intermolecular exchange interaction.

Experimental Section

The synthesis and physical properties of Nit(SMe)Ph have been reported elsewhere.[19] The room-temperature structure for Nit(SMe)Ph is known from X-ray analysis.[19] The corresponding crystal data are reported in Table 1. Large crystals, suitable for neutron experiments, were obtained by slow evaporation of a hexane and $CHCl_3$/heptane solution.

Table 1. Crystal data of Nit(SMe)Ph at room temperature.

space group	$P2_1/a$	V[Å^3]	1459.5(5)
a[Å]	9.437(2)	β[°]	113.66(2)
b[Å]	19.827(2)	Z	4
c[Å]	8.516(2)		

Low-temperature structure refinement: A single crystal, in the form of a regular slab of dimensions $5.0 \times 1.7 \times 1.5$ mm^3, was used for the neutron experiment. The unpolarised neutron diffraction experiment was performed on the D15 diffractometer at the ILL reactor (Grenoble, France). The sample was cooled to 10 K, and 2456 reflections were collected with $\sin\theta/\lambda \leq 0.80$ Å^{-1} ($\lambda = 1.173$ Å). Crystal data and experimental parameters at $T = 10$ K are reported in Table 2.

The calculation of the integrated intensities from the ω scans was performed by the COLL5 program[21] during the experimental run-time.

Table 2. Crystal data and experimental parameters for the unpolarised neutron experiment of Nit(SMe)Ph.

space group	$P2_1/a$	T[K]	10
a[Å]	9.236(26)	neutron wavelength[Å]	1.173
		$\sin\theta/\lambda_{max}$[Å^{-1}]	0.80
b[Å]	19.393(13)	no. of measured reflections	2456
c[Å]	8.603(8)	no. of independent reflections	1061
β [°]	114.94(12)	χ^2	1.4
$R_w(F)$	0.044		

The program ARRNGE, based on the Cambridge Crystallographic Library,[22] was used to average the equivalent reflections. The absorption coefficient $\mu = 0.212\ mm^{-1}$ was obtained by assuming $\sigma = 38$ barn for the hydrogen atoms of the molecule. It was then used to calculate the absorption correction by estimating the mean crystal path for each (hkl) reflection collected. Refinement of the atomic position from room-temperature values was carried out with the least-square program ORXFLS[23] with anisotropic thermal factors for all atoms. Extinction turned out to be significant. It was modelled in the approximation of a Gaussian mosaic crystal.[24] In this framework, Equation (2) was used for the scattering intensity corresponding to secondary type II extinction.

$$I = F^2 G(I^0), \text{ with } G(I^0) = \frac{1}{\sqrt{1 + \frac{2gL\lambda^3}{V^2 \sin(2\theta)} F^2}} \quad (2)$$

I^0 is the "kinematic" intensity, V the unit cell volume and L, the mean crystal traversing path. The value of the coefficient g was refined together with the crystal structure ($g = 51.3(2)$ with L, λ, V and F^2 in cm, Å, Å^3 and 10^{-24} cm^2, respectively).

The refinement statistics are also given in Table 2. Selected interatomic distances and bond angles are given in Table 3.

Table 3. Selected low-temperature bond lengths [Å] and bond angles [°].

S1−C5	1.745(5)	S1−C14	1.803(9)	N1−O1	1.270(3)
N2−O2	1.275(3)	N1−C1	1.349(2)	N1−C8	1.508(2)
N2−C1	1.358(3)	N2−C9	1.498(3)	C1−C2	1.450(3)
C2−C3	1.395(5)	C2−C7	1.406(4)	C3−C4	1.391(3)
C4−C5	1.390(3)	C5−C6	1.396(6)	C6−C7	1.385(3)
C8−C9	1.555(5)	C8−C10	1.542(7)	C8−C12	1.521(3)
C9−C11	1.520(8)	C9−C13	1.521(4)		
C5-S1-C14	102.7(3)	O1-N1-C1	127.2(2)	O1-N1-C8	121.1(2)
C1-N1-C8	111.4(2)	O2-N2-C1	126.5(2)	O2-N2-C9	121.3(2)
C1-N2-C9	112.1(2)	N1-C1-N2	108.9(2)	N1-C1-C2	126.5(2)
N2-C1-C2	124.5(2)	C1-C2-C3	119.0(3)	C1-C2-C7	122.0(3)
C3-C2-C7	118.7(2)	C2-C3-C4	120.6(3)	C3-C4-C5	120.5(4)
S1-C5-C4	125.3(4)	S1-C5-C6	115.8(3)	C4-C5-C6	118.9(3)
C5-C6-C7	120.9(3)	C2-C7-C6	120.1(4)	N1-C8-C9	101.1(2)
N1-C8-C10	105.7(3)	N1-C8-C12	109.8(2)	C9-C8-C10	113.3(3)
C9-C8-C12	115.1(4)	C10-C8-C12	110.9(3)	N2-C9-C8	101.0(3)
N2-C9-C11	106.5(3)	N2-C9-C13	109.5(3)	C8-C9-C11	112.6(3)
C8-C9-C13	115.4(4)	C11-C9-C13	111.0(4)		

Polarised neutron experiment: The polarised neutron investigation of the Nit(SMe)Ph free radical was performed on two crystals. Firstly on the same crystal as that used in the unpolarised neutron diffraction experiment (crystal **1**), and then on a single crystal of dimensions $3.5 \times 2.5 \times 1.5\ mm^3$ (crystal **2**). This experiment was performed on the DN2 polarised neutron diffractometer at the SILOE reactor (Grenoble, France) with an incident wavelength $\lambda = 1.205$ Å. Crystal **1** was mounted with the a axis vertical (parallel to the applied $H = 8$ T magnetic field of a cryomagnet). The diffractometer was equipped with a lifting counter which enabled the measurement of several layers of reflections in the reciprocal space: reflections of type ($0kl$), ($1kl$) and ($2kl$). Crystal **2** was mounted with the c axis parallel to the applied magnetic field ($H = 8$ T) and reflections of type ($hk0$), ($hk1$) and ($hk2$) were measured. In both series the sample temperature was kept at 5.3 K. Altogether 357 independent flipping ratios were collected with $\sin\theta/\lambda \leq 0.55$ Å^{-1}.

Precise nuclear structure factors were calculated from the refined low-temperature crystal structure. The subroutine library mentioned above[22] was used to sort and average the equivalent flipping ratios. The expression in Equation (1) for the flipping ratio was modified to include corrections which result from the imperfection of the beam and from extinction. The magnetic structure factors were determined from this modified expression.

Results

Structural study: Figure 1 shows the molecule of Nit(SMe)Ph with the atom-labelling scheme used here. Figures 2 and 3 show the packing of the molecules along the a axis and the shortest intermolecular contacts relevant to the magnetic properties, respectively. At low temperature, the crystal symmetry of Nit(SMe)Ph is preserved and no drastic changes in the cell constants are observed compared to room temperature (Tables 1 and 2). The phenyl ring is twisted around the C1−C2 bond by 30.7° (32.2° at room temperature) with respect to the O-N-C-N-O plane. In NitPh the range of the corresponding angle is 25–30°. The global intermolecular arrangement of the molecules in the crystal is also preserved when the temperature changes from 300 K to 10 K. Therefore, we only discuss the points which are relevant to the spin-density results. i) The unit cell contains four free radical molecules which are arranged in pairs. These pairs form a two-dimensional network perpendicular to the b axis (Figure 2). ii) Short intermolecular contacts are found between the NO

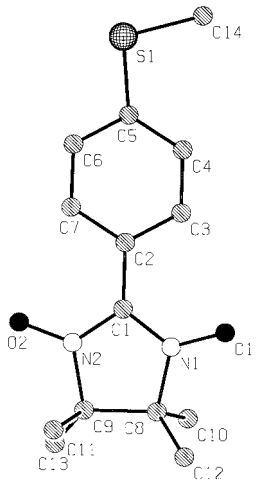

Figure 1. View of the Nit(SMe)Ph molecule showing the numbering scheme of the atoms.

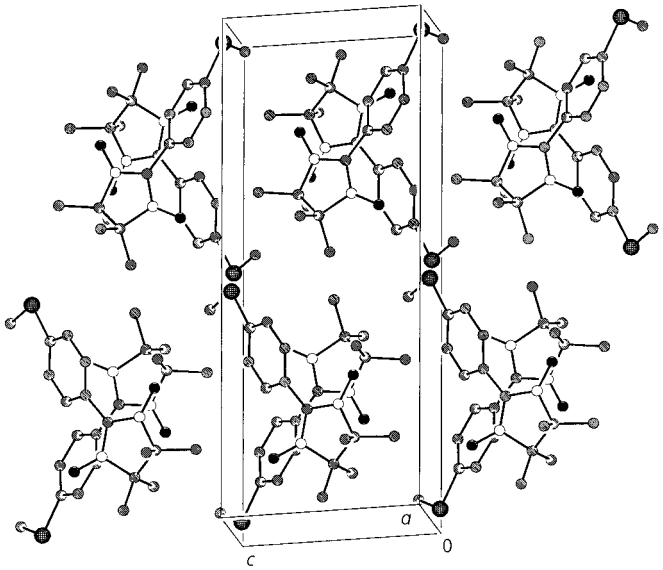

Figure 2. View of the crystal packing of Nit(SMe)Ph along the a axis.

0947-6539/99/0512-3618 $ 17.50+.50/0 *Chem. Eur. J.* **1999**, *5*, No. 12

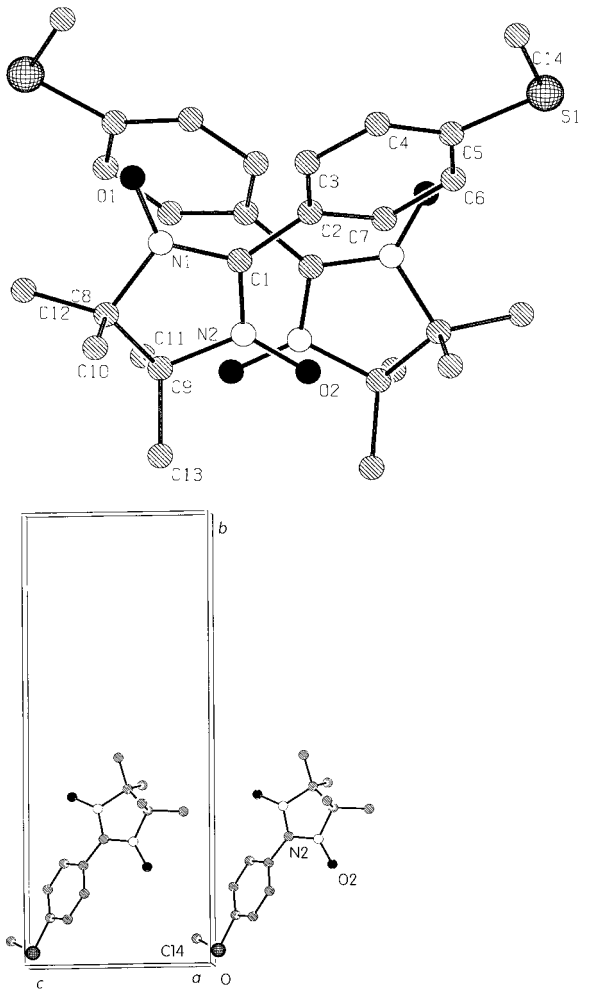

Figure 3. Short intermolecular distances between molecules related by the glide plane $x+1/2,\ 1/2-y,\ z$ (top), and between molecules related by the translation along the c axis (bottom).

group (N1O1) of a molecule and the phenyl carbon atoms (C2′ to C7′) of the molecule related by the glide planes $x+1/2,\ -y+1/2,\ z$ and $x-1/2,\ -y+1/2,\ z$ (Figure 3a; distances in the range 3.65–4.37 Å). Intermolecular contacts between the two NO groups (N2O2 and N2′O2′) of molecules related by the same symmetry operation are also found (Figure 3a; distances in the range 4.35–4.76 Å). iii) Another weak intermolecular contact (3.72 Å) is found between the NO group of the molecule of the asymmetric unit and the C14′ carbon atom of the methylthio group of a molecule related by a translation along the c axis ($x, y, z-1$, Figure 3b).

Spin-density reconstruction: The magnetic structure factors are the Fourier components of the spin density $M(\vec{r})$. Reconstruction of spatial spin density from the experimental magnetic structure factors is a typical Inverse Fourier (IF) problem. The IF problem was solved within the limitations of accuracy and completeness of polarised neutron diffraction data. In these experiments, the data are noisy, the error bars are uneven, the sampling of data points in reciprocal space is somewhat arbitrary, and the spatial resolution of the diffraction experiment is limited. Therefore, several approaches were used to solve the IF problem.

Reconstruction based on the modelling of the spin density: A possible approach is to design a parameterised model of the spin-density distribution and refine the parameters which give the best fit with the experimental data. To obtain individual spin populations of the complete molecule, we used the magnetic wave function refinement method.[18] In this framework an LCAO-like magnetic wave function $|\Psi_i\rangle$ was constructed from the standard Slater atomic orbitals $|\Phi_{ij}\rangle$ at each atomic site i [Eq. (3)], where j labels the atomic Slater wave functions of an atom i, and $\alpha_{i,j}$ are the expansion coefficients, which are scaled to give $\langle\Psi_i|\Psi_i\rangle=1$. The spin density $S(\vec{r})$is then expanded according to Equation (4).

$$|\Psi_i\rangle=\sum_j \alpha_{i,j}|\Phi_{ij}\rangle \tag{3}$$

$$S(\vec{r})=\sum_i S_i\Psi_i(\vec{r})\Psi_i^*(\vec{r}) \tag{4}$$

The individual atomic spin populations S_i as well as the coefficient $\alpha_{i,j}$ and the radial exponents, ζ, of the Slater wave functions for each orbital type are the model parameters which were refined to best fit the data.

In our refinement, we have included the $|2s\rangle$, $|2p_x\rangle$, $|2p_y\rangle$ and $|2p_z\rangle$ orbitals at the O1, N1, N2 and O2 atomic sites,[25] to yield $|\Phi\rangle=\alpha_1|2s\rangle+\alpha_2|2p_x\rangle+\alpha_3|2p_y\rangle+\alpha_4|2p_z\rangle$, $(\alpha_1^2+\alpha_2^2+\alpha_3^2+\alpha_4^2=1$. A $|2p_z\rangle$ orbital was included at the C1 atomic site (z axis is perpendicular to the O-N-C-N-O mean plane). The spin density on the other atoms is weak and is reduced to its spherical contributions.

The model was refined with a modified least-squares program MOLLY.[26] The starting values of the Slater radial exponents were taken from literature.[27] They were refined for N and O atoms where the spin density is mainly located.

The resulting populations are presented in Table 4 along with the refinement statistics. The refined radial exponents ζ are given in Table 5. Table 6 shows the refined $\alpha_{i,j}$ coefficients for the orbitals on the O1, N1, N2 and O2 atomic sites. Figure 4 shows the contours for the spin density projected

Table 4. Atomic spin populations corresponding to $T=5.3$ K, $H=8$ T.[a,b]

Atoms	Spin populations (μ_B)	Atoms	Spin populations (μ_B)
O1	0.194(6)	N1	0.233(8)
O2	0.194(7)	N2	0.212(8)
S1	0.001(6)	C1	−0.085(7)
C2	−0.021(8)	C3	0.003(8)
C4	0.016(6)	C5	−0.018(7)
C6	0.027(6)	C7	0.001(6)
C8	−0.014(7)	C9	0.001(8)
C10	0.022(6)	C11	0.018(6)
C12	0.019(5)	C13	0.028(7)
C14	0.027(6)		

[a] Statistics of the wave-function refinement: no. of variables = 38; no. of independent F_M values = 357; $\chi^2/N_{obs}=1.45$. [b] Sum of spin population = 0.858(7).

Table 5. Refined Slater radial exponents, wave-function modelling.

ζ(O) initial value	2.25	ζ(N) initial value	1.95
ζ(O) refined value	2.85(7)	ζ(N) refined value	1.99(4)
ζ(C) not refined	1.72	ζ(S) not refined	1.80

Table 6. Refined wave function coefficients.

Atoms	$\alpha_1(\|2s\rangle)$	$\alpha_2(\|2p_x\rangle)$	$\alpha_3(\|2p_y\rangle)$	$\alpha_4(\|2p_z\rangle))$
O1	0.158(36)	0.430(114)	−0.126(112)	0.880
N1	0.035(44)	−0.082(115)	−0.228(144)	0.970
N2	−0.045(54)	0.062(120)	0.132(120)	0.989
O2	−0.197(42)	−0.058(89)	0.482(122)	0.852

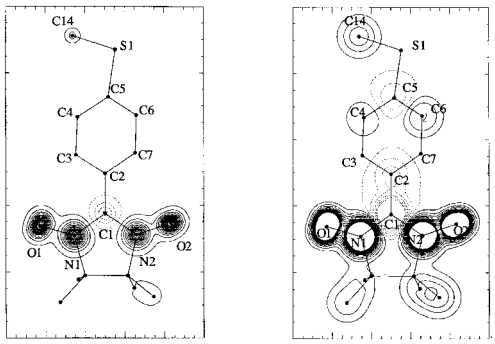

Figure 4. Projection of the spin density as analysed by wave-function modelling onto the nitroxide mean plane (Nit(SMe)Ph). Negative contours are dashed: Left: high-level contours (step 0.04 μ_B Å^{-2}); right: low-level contours (step 0.006 μ_B Å^{-2}).

onto the O-N-C-N-O fragment. A projection of the reconstructed spin density onto a plane perpendicular to the O-N-C-N-O plane and parallel to the N–N direction is shown in Figure 5. A perspective visualisation of the spin density of the complete molecule is represented in Figure 6.

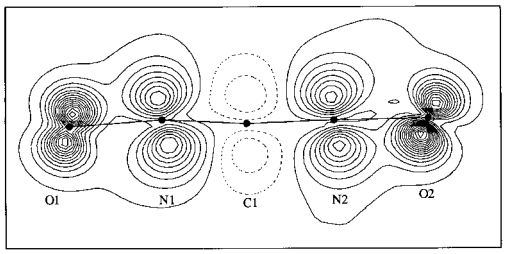

Figure 5. Projection of the contours (step 0.03 μ_B Å^{-2}) of the spin density onto a plane perpendicular to the nitroxide mean plane, as analysed by wave-function modelling (Nit(SMe)Ph). Negative contours are dashed.

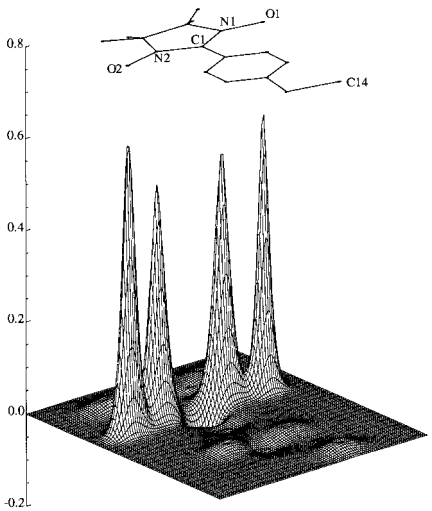

Figure 6. Perspective view of the spin density (Nit(SMe)Ph radical) reconstructed by wave-function modelling.

Several important features are worthy of mention: i) as expected for this type of compounds, the largest spin populations are carried by the O1-N1-C1-N2-O2 fragment (Figure 5), and the partitioning of the O1, N1, N2 and O2 spin populations is approximately 1:1:1:1. ii) As previously[20] determined, the central carbon atom C1 carries a negative spin density. The ratio of its spin population to the average of the spin populations of the O1, N1, N2 and O2 atoms is approximately −1/3. iii) A strong and significant rotation and hybridisation of the magnetic molecular orbital of the O1 and O2 oxygen atoms were found (Table 6, Figure 5). The equivalent effect was not significant on the N1 and N2 atoms. iv) Some significant spin density was obtained outside the nitroxide heterocycle: on the C2 (−0.021(8) μ_B), C4 (0.016(6) μ_B), C5 (−0.018(7) μ_B) and C6 (0.027(6) μ_B) carbon atoms of the phenyl ring; on the C14 (0.027(6) μ_B) carbon atom of the methylthio group. Practically no spin density was detected on the sulphur atom S1 ((0.001(6) μ_B).

Model-independent reconstruction: An alternative approach is to use a model-independent method in order to reconstruct the spin density without involving any a priori knowledge of what the spin density should look like. The most straightforward approach to solving the IF problem is to calculate the inverse Fourier sum [Eq. (5), where V is the unit cell volume.

$$S(x,y,z) = 1/V \sum_{h,k,l} F_M(h,k,l) e^{-2\pi i(hx+ky+lz)} \quad (5)$$

This sum should be extended in principle to all the nodes (hkl) of the reciprocal lattice; however, it is actually limited to the Bragg reflections for which the F_M values were determined. This method has been widely used to interpret polarised neutron diffraction data,[28] although it has its drawbacks. Since not all Fourier components are known, there are in fact many possible spin density maps which fit the data. Fourier inversion selects one of them—the one with zero values for unmeasured coefficients and values exactly in the middle of the error bars for those measured. In contrast, the maximum entropy (ME) technique[29a] selects the most probable map from all those which are consistent with the data, that is the one which maximises the Boltzman entropy [Eq. (6)].

$$\text{entropy}(S(\vec{r})) = -\int_{\text{unit cell}} s(\vec{r}) \ln(s(\vec{r})) \mathrm{d}^3\vec{r}$$
$$s(\vec{r}) = \frac{S(\vec{r})}{\int_{\text{unit cell}} S(\vec{r}) d^3\vec{r}} \quad (6)$$

This formula strictly applies to positive densities; however, the method has been modified to treat sign-alternated densities.[29b] In practice one maximises the functional [Eq. (6)] calculated for a three-dimensional spin density map under the constraint $\chi^2 \leq 1$. A projection along the desired direction is obtained directly by integration of the three-dimensional distribution. This method has been shown[29a] to give much better results than conventional Fourier inversion and is also model-independent.

The spin-density map was reconstructed with a program based on the MEMSYS subroutine package.[30] Figure 7 shows the projection of this density onto the O-N-C-N-O molecular

  0947-6539/99/0512-3620 $ 17.50+.50/0 *Chem. Eur. J.* **1999**, *5*, No. 12

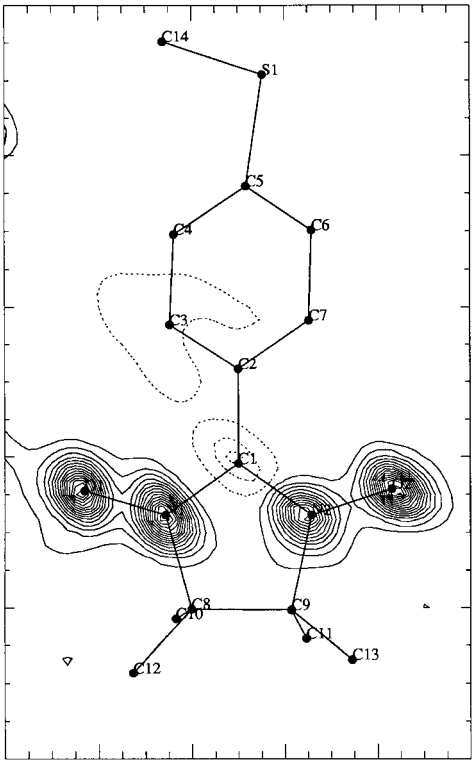

Figure 7. Projection of the ME-reconstructed spin density onto the nitroxide mean plane of the Nit(SMe)Ph molecule. Negative contours are dashed, contour step 0.02 μ_B Å^{-2}.

plane. As previously described, the main part of the spin density is located on the two NO groups and is approximately equally shared by the oxygen and nitrogen atoms. The bridging sp^2 C1 carbon atom carries a negative spin density.

No spin density is detected by this method on atoms of the carbon skeleton; however, this cannot be used as evidence for the absence of spin population on these sites as ME usually does not detect the small contributions to the spin density.

At this stage, it is interesting to check the reality of the effects determined with the wave function modelling and particularly the rotation and the hybridisation of the magnetic molecular orbital of the two oxygen atoms O1 and O2 of the NO groups. It is possible to use the new method of spin-density reconstruction which includes the advantages of the traditional ME described above and wave-function modelling:[31] ME reconstruction with an atomic orbital default model (DMME). This method is based on the extended entropic functional introduced by Skilling [Eq. (7)].[32]

$$\text{entropy}(S(\vec{r})) = -\int_{\text{unit cell}} s(\vec{r})\left(1-\ln\left(\frac{s(\vec{r})}{m(\vec{r})}\right)d^3\vec{r}\right) \qquad (7)$$

As with traditional ME, it allows unlimited freedom of the spin-density distribution and always yields a density map which corresponds to $\chi^2 \leq 1$. In addition, it allows the introduction of a priori information into the treatment of the data: the "default model" of spin density $m(\vec{r})$. It only influences the entropic functional, that is only the way the best map is chosen from among those consistent with the data. The "default model" does not in any way restrict the density map itself. If the data are compatible with the default model, the DMME result will be identical to the model. On the contrary, if the data are not compatible, the spin density reconstructed with DMME will be the one which resembles the model as much as possible and still fits the data. In this case, any deviation of the reconstructed density from the model is contained in the experimental data, since it costs entropy.

We used a default model with a symmetric arrangement of the $|2p_z\rangle$ orbitals on the O1, N1, C1, N2 and O2 atoms (whereby z is perpendicular to the O-N-C-N-O plane), as shown in Figure 8 (top). The DMME-reconstructed spin-density map is presented in Figure 8 (bottom).

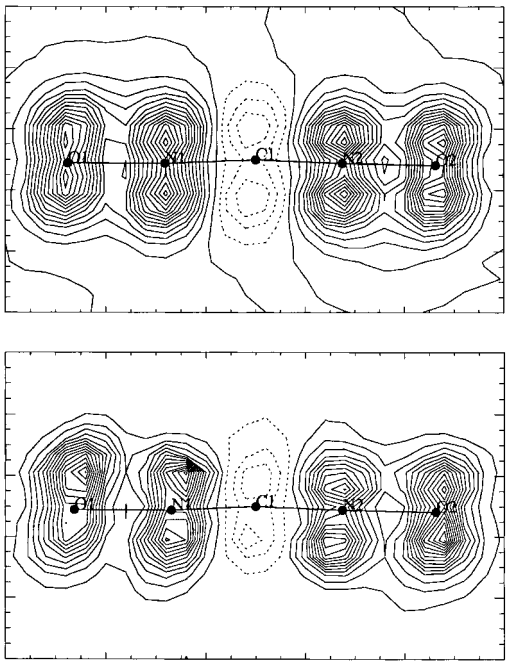

Figure 8. Projection of the spin density (contour step 0.015 μ_B Å^{-2}) onto a plane perpendicular to the nitroxide mean plane: top) the default model; bottom) the DMME-reconstructed spin density. Negative contours are dashed.

It is apparent that the rotation and the hybridisation of the magnetic molecular orbital of the two oxygen atoms O1 and O2 are really contained in the experimental data. If the magnetic orbitals of the N1, C1 and N2 atoms are practically perpendicular to the O-N-C-N-O plane (as determined by wave-function modelling), those of the O1 and O2 oxygen atoms form an angle with the z axis and a lobe of each orbital is stronger than the other (hybridisation). The latter effects are consistent with those determined by wave-function modelling. In both cases, the rotation is in the same direction and it is the same lobe of each orbital which is inflated.

As a conclusion to the spin-density reconstruction, we can say that the different approaches converge and show, on the one hand, that the major part of the spin density of Nit(SMe)Ph should be attributed to the unpaired electron residing on the singly occupied molecular orbital (SOMO) which is constructed on the $|2p\rangle$ atomic orbitals of the O1, N1, N2 and O2 atoms, and on the other hand, that the 2p orbitals on both oxygen atoms O1 and O2 are rotated and hybridised.

Ab initio spin-density calculations: Having obtained the accurate polarised neutron diffraction data, we performed theoretical calculations. Several methods of calculation can be used. The classical unrestricted Hartree–Fock (UHF) method, the UHF-based methods (Møller–Plesset perturbation theory (MP-2, MP-3, etc.),[33] the configuration interaction (CI) method[34]) and functional density theory (DFT) method.[35] UHF, MP-2, CI and DFT calculations of spin density in NitPh have already been reported.[20] The main conclusion is that UHF-based methods cannot be trusted for the calculation of the spin densities of organic free radicals. Therefore, for our spin density calculations, we have applied the DFT method as implemented in the program DGAUSS.[36] At the local spin-density functional level, the functional of Vosko, Wilk and Nusair[37] was used, with nonlocal correlational potential of Perdew'86[38] and the nonlocal exchange potential of Becke'88.[39] The DGAUSS program uses Gaussian basis sets. The different calculations were performed with local density-optimised basis sets at the DZVP and TZVP levels for molecules in their experimental low-temperature crystal geometry. Firstly, the spin distribution of an isolated molecule of Nit(SMe)Ph was calculated. Then, to check the effect of the crystal packing in the Nit(SMe)Ph radical, we have calculated the spin populations of two molecules connected by the short intermolecular contact presented in Figure 3b (C14′⋯O2–N2). In both cases, the results obtained with DZVP and TZVP basis sets are practically the same. Consequently we present below only the Mulliken spin populations calculated with the DZVP basis set.

An isolated molecule: The individual atomic spin populations of an isolated molecule of Nit(SMe)Ph, calculated with the DZVP basis set, are listed in Table 7 together with the experimental values. The latter are scaled to 1 μ_B molecule. The spin populations obtained on the nitroxide ring are of the same order of magnitude as the experimental values. The main difference lies in the O:N population ratio: the calculated value was 30:22 as opposed to 23:26 determined experimentally. Additionally, some spin delocalisation was found on the carbon atoms of the phenyl ring. The sign of the calculated polarisations are consistent with those determined experimentally, except for the C2 carbon atom; however, the values calculated are much smaller than those measured: the calculated/experimental spin population ratios are 0.005/–0.024(9), 0.002/0.019(7), –0.007/–0.021(8) and 0.002/0.031(9) μ_B for C2, C4, C5 and C6 atomic sites, respectively. Finally, no spin density was found on the terminal carbon atom C14 of the methylthio group.

Table 7. Theoretical atomic spin populations calculated (DFT) for an isolated molecule in comparison with those determined experimentally.[a]

Atoms	DZVP Spin populations [μ_B]	Experimental spin populations scaled to 1 μ_B
O1	0.304	0.226(7)
O2	0.308	0.226(8)
N1	0.221	0.272(9)
N2	0.225	0.247(9)
S1	–0.004	0.001(7)
C1	–0.063	–0.099(8)
C2	0.005	–0.024(9)
C3	–0.010	0.003(9)
C4	0.002	0.019(7)
C5	–0.007	–0.021(8)
C6	0.002	0.031(7)
C7	–0.008	0.001(7)
C8	–0.006	–0.016(8)
C9	–0.005	0.001(9)
C10	0.017	0.026(7)
C11	0.016	0.021(7)
C12	0.002	0.022(6)
C13	0.003	0.033(8)
C14	0.000	0.031(7)

[a] Values are scaled to 1 μ_B per Nit(SMe)Ph formula.

Two molecules in contact: Table 8 gives the calculated spin populations (DZVP basis set) of the O1-N1-C1-N2-O2 group of the molecule of the asymmetric unit and of the C14′ carbon atom of a second molecule related by x, y, $z-1$. The corresponding spin populations of an isolated molecule, together with experimental values, are also presented in Table 8. The main information to extract from these results is the weak "transfer" of spin density from the O2 oxygen atom to the C14′ carbon atom. Otherwise, a small depletion is observed on the O2 oxygen atom of the O-N-C-N-O fragment between the "isolated" molecule and the "interacting" molecule.

Table 8. DFT values of the atomic spin populations calculated for an isolated molecule and for two molecules related by $x, y, z-1$ in comparison with the experimental values scaled to 1 μ_B per Nit(SMe)Ph formula.

Atoms	DZVP isolated molecule	DZVP two molecules	Experimental spin populations [μ_B]
O1	0.304	0.307	0.226(7)
N1	0.221	0.221	0.272(9)
C1	–0.063	–0.063	–0.099(8)
N2	0.225	0.229	0.247(9)
O2	0.308	0.298	0.226(8)
C14	0.000	0.001	0.031(7)

Discussion

The most relevant feature of the spin-density distribution of Nit(SMe)Ph emerges from the comparison with that of NitPh. In fact, if we compare the spin density of the O1-N1-C1-N2-O2 fragment in the two radicals, it appears that almost all the spin density is located on this fragment in NitPh (0.969 μ_B[20]), while this value is equal to only 0.877 μ_B for the Nit(SMe)Ph radical. This may be taken as evidence that the magnetic coupling between the Nit(SMe)Ph molecules implies a noticeable delocalisation of the spin density out of the O-N-C-N-O fragment.

A further difference between the two radicals concerns the shape of the experimental spin density on the O1 and O2 atoms of the two NO groups. In fact, in Nit(SMe)Ph a marked deviation from the spin density which would be associated with the $2p_z$ orbital is observed, suggesting that this may be the result of interactions with orbitals of neighbouring molecules. Therefore, there is a strong indication that these alterations in the geometry of the spin density in Nit(SMe)Ph must be connected to the intermolecular magnetic coupling.

0947-6539/99/0512-3622 $ 17.50+.50/0 *Chem. Eur. J.* **1999**, *5*, No. 12

The O-N-C-N-O spin populations obtained by DFT calculations are of the same order of magnitude as those determined experimentally. However, there are two main differences: firstly, the DFT method fails to predict the O:N spin occupancies, and yields a value of ≈3:2 compared to the experimental value of ≈1:1. This effect has already been observed in other nitronyl nitroxide free radicals independent of the employed functional, basis set and population analysis.[20] Secondly, as shown in Table 8, the sum of the spin populations on the O-N-C-N-O atoms amounts to 0.995 μ_B with DFT calculations, which indicates that almost all the spin density is localised on that fragment, while the experimentally determined value of the sum is 0.877 μ_B.

As far as the methylthiophenyl group is concerned, several features need to be emphasised. i) The alternating …+/−/+/−… spin population of the phenyl ring atoms, which is generally observed in this class of compound where the angle between the phenyl ring and the O-N-C-N-O plane is not too large (≤30°), is not completely respected. The experimental negative spin density on the C2 carbon atom (−0.024(9) μ_B) breaks this alternation. This anomalous alternation of spin density within the benzene ring is surprising, but not unexpected. In fact, similar results have been reported by NMR studies of sterically hindered nitroxide radicals.[40] Of greater interest is the total shift of the spin density on the aromatic fragment towards the methylthio group: the C4 and C6 spin populations (0.019(7) μ_B and 0.031(7) μ_B, respectively) are an order of magnitude larger than those of C3 and C7 (0.003(9) μ_B and 0.001(7) μ_B, respectively). Moreover, the C5 atom, which is bonded to C4 and C6, carries a strong and significant negative spin density. The carbon atoms which have higher spin densities are those which present short intermolecular contacts with the N1O1 group. ii) As regards the methylthio group, only the C14 atom carries a significant spin density (≈ +13% of the average of the O1, N1, N2 and O2 spin populations).

DFT calculations provide evidence for the existence of some spin density on the phenyl ring (spin delocalisation) in the isolated molecule; however, no density is calculated on the C14 atom. When two molecules are connected by the C14···O2 contact, some *positive* spin density is obtained on the C14 atom. Thus, this positive spin density probably comes from the interaction between adjacent molecules by means of a transfer of spin density from the N2O2 group towards the C14 atom. Therefore, there is a qualitative indication that this contact may be responsible for the ferromagnetic coupling between the Nit(SMe)Ph molecules, even if the DFT method fails to predict the experimental spin density quantitatively. The calculated/observed spin density ratio of C14 is 1:31.

The experimental determination of the distribution of unpaired spin density in this radical provides some answers concerning the pathways of intermolecular ferromagnetic interactions. First of all it rules out the pathway that was suggested previously,[19] which took into account the interactions through the S atoms. In fact these induce a negligibly small unpaired spin density on this atom, and therefore they must be discarded. On the other hand, there is a significant interaction between the NO groups and the C14 atom, which suggests that the coupling mechanism must involve these groups. Interestingly, this pathway is in agreement with the EPR data that suggested that the pathway went through the SMe groups. The neutron data seem to simply suggest a different pathway within the SMe group.

If the neutron data provide some hints on the exchange pathway, the problem is still open on the nature of the exchange mechanism.

Two different mechanisms, which associate magnetic interactions between organic radicals to particular intermolecular contacts, have been given by Harden M. McConnell.[41, 42] The so-called McConnell's I mechanism establishes that ferromagnetic (antiferromagnetic) coupling arises from intermolecular contacts between atoms that carry spin populations of opposite (equal) signs. In the second mechanism (McConnell's II mechanism), the ferromagnetic coupling arises from SOMO–LUMO contacts between adjacent molecules, while the antiferromagnetic coupling is explained in terms of SOMO–SOMO contacts between two radicals.

In the present case, a possible explanation for the sign of the magnetic interaction can be given by considering the SOMO and LUMO orbitals for both molecules (Figure 9). Note that

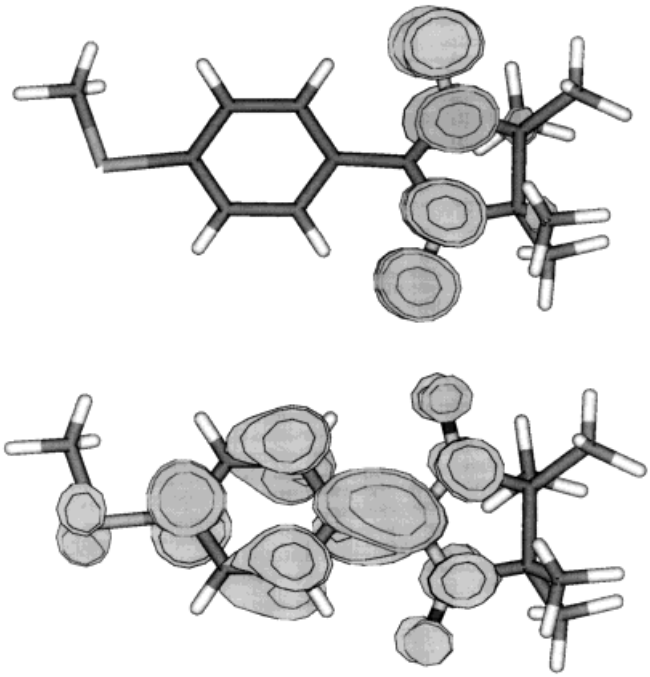

Figure 9. SOMO (top) and LUMO (bottom) orbitals of the Nit(SMe)Ph radical obtained by DFT calculations.

the LUMOs are distributed throughout the methylthio fragment with a significant contribution on the S atom. According to the nature of the exchange pathway and to the increased unpaired spin density on the (SMe)Ph group, the main role of the S1−C14···O2−N2 contact is then to promote an overlap between SOMO and LUMO orbitals that belong to neighbouring molecules while avoiding intermolecular SOMO–SOMO contacts. This results in a net ferromagnetic interaction, according to McConnell's II mechanism.

Conclusions

The determination of spin-density distributions through polarised neutron diffraction experiments, coupled to DFT calculations, can shed light on the mechanism of exchange interactions between radicals. The present results ruled out the strategy of the use of soft atoms, such as sulfur, to establish efficient ferromagnetic coupling between Nit radicals; however, it showed that contacts between the NO groups and seemingly unattractive groups, such as CH_3, may be enough to give rise to bulk magnetic properties. It must be stressed, however, that the suggested efficient contact is responsible for the relatively high-temperature magnetic behaviour of Nit(SMe)Ph. The exact nature of the weaker interaction responsible for the T_c remains undefined.

Finally, DFT calculations have confirmed that the CH_3 group of the methylthio fragment is involved in the intermolecular exchange pathway. However, there is still a large discrepancy between the experimental and the quantitative DFT results.

Acknowledgements

The financial support by MURST and TMR grant 3MD (No. ERB 4061 PL 97-0197) is gratefully acknowledged.

[1] T. J. Stone, P. L. Buckman, P. L. Nordio, H. McConnell, *Proc. Natl. Acad. Sci USA.* **1965**, 54, 1010.
[2] *Spin labeling Vol. 1*, *Vol. 2* (Ed.: L. D. Berliner), Academic Press, New York, **1976**, **1979**.
[3] E. G. Rozantsev, *Free Nitroxyl Radicals*, Plemum Press, New York, **1970**.
[4] J. F. Keana, *Chem. Rev.* **1978**, *78*, 37.
[5] J. H. Osiecky, E. F. Ullman, *J. Am. Chem. Soc.* **1968**, *90*, 1078.
[6] K. Awaga, T. Inabe, T. Okayama, Y. Maruyama, *Mol. Cryst. Liq. Cryst.* **1993**, *232*, 79.
[7] K. Awaga, T. Inabe, Y. Maruyama, *Chem. Phys. Lett.* **1992**, *190*, 349.
[8] K. Awaga, T. Inabe, Y. Maruyama, T. Nakamura, M. Matsumoto, *Chem. Phys. Lett.* **1992**, *195*, 21.
[9] T. Sugano, M. Tamura, M. Kinoshita, Y. Sakai, Y. Ohashi, *Chem. Phys. Lett.* **1992**, *200*, 235.
[10] P. Turek, K. Nozawa, D. Shiomi, K. Awaga, T. Inabe, Y. Maruyama, M. Kinoshita, *Chem. Phys. Lett.* **1991**, *180*, 327.
[11] Y. Hosokoshi, M. Tamura, M. Kinoshita, *Mol. Cryst. Liq. Cryst.* **1993**, *232*, 45.
[12] M. Kinoshita, P. Turek, H. Tamura, K. Nozana, D. Shiomi, Y. Nakazama, M. Ishikawa, M. Takahashi, K. Awaga, T. Inabe, Y. Muzuyama, *Chem. Lett*. **1991**, 1225.
[13] K. Awaga, Y. Maruyama, *Chem. Phys. Lett.* **1989**, *158*, 556.
[14] K. Awaga, T. Inabe, U. Nagashima, Y. Maruyama, *J. Chem. Soc. Chem. Commun.* **1989**, 1617.
[15] T. Sugawara, M. M. Matsushita, A. Izuoka, N. Wada, N. Takeda, M. Ishikawa, *J. Chem. Soc. Chem. Commun.* **1994**, 1723; J. Cirujeda, M. Mas, E. Molins, F. Lanfranc de Panthou, J. Laugier, J. G. Park, C. Paulsen, P. Rey, C. Rovira, J. Veciana, *J. Chem. Soc. Chem. Commun*. **1995**, 709; F. Romero, R. Ziessel, M. Drillon, J.-L. Tholence, N. Kyritsakas, J. Fisher, *Adv. Mater.* **1996**, 8, 826.
[16] R. Chiarelli, M. A. Novak, A. Rassat, J.-L. Tholence, *Nature*, **1993**, *363*, 147.
[17] M. Deumal, J. Cirujeda, J. Veciana, J. J. Novoa, *Adv. Mater*. **1998**, *10*, 1461.
[18] B. Gillon, J. Schweizer, "Study of Chemical Bonding in Molecules" in *The interest of Polarised Neutron Diffraction. In Molecules in Physics, Chemistry and Biology, Vol. II* (Ed.: J. Maruani), Kluwer, Dordrecht (The Netherlands), **1989**, p. 111.
[19] A. Caneschi, F. Ferraro, D. Gatteschi, A. Le Lirzin, E. Rentschler, *Inorg. Chem. Acta* **1994**, *217*, 7.; A. Caneschi, F. Ferraro, D. Gatteschi, A. Le Lirzin, M. Novak, E. Rentschler, R. Sessoli, *Adv. Mater.* **1995**, *7*, 476.
[20] A. Zheludev, V. Barone, M. Bonnet, B. Delley, A. Grand, E. Ressouche, P. Rey, R. Subra, J. Schweizer, *J. Am. Chem. Soc.* **1994**, *116*, 2019.
[21] M. S. Lehmann, F. K. Larsen, *Acta Crystallogr. Sect. B 26*, **1970**, 1198.
[22] P. J. Brown, J. C. Mattheman, *The Cambridge Crystallographic Subroutine Library* RL-81-063.
[23] W. R. Busing, K. O. Martin, H. Levy, A. Rapport, *O.R.N.L. 59–37*, Oak Ridge National Laboratory, Oak Ridge, TN, **1991**.
[24] P. Coppens, W. C. Hamilton, *Acta Crystallogr. Sect. A*, **1970**, *26,* 71.
[25] Our definition of the *x*, *y*, and *z* coordinate system: *z* axis is perpendicular to the O-N-C-N-O plane, *x* axis is along the C1 – C8 direction for O1 and N1 atoms and along the C1 – C9 direction for O2 and N2 atoms.
[26] N. K. Hansen, P. Coppens, *Acta Crystallogr. Sect. A*, **1978**, *34*, 909.
[27] N. J. Hehre, R. F. Stewart, J. A. Pople, *J. Chem. Phys.* **1969**, 51.
[28] First application: C. G. Shull, Y. Yamada, *J. Phys. Soc. Jap.* 17 Suppl. BIII, **1962**, 1; a more recent example: J. X. Boucherle, F. Givord, P. Lejay, J. Schweizer, A. Stunault, *Physica B*, **1989**, 809.
[29] a) S. F. Gull, G. J. Daniell, *Nature*, **1978**, *272*, 686; b) R. J. Papoular, B. Gillon, *Europhys. Lett.* **1990**, *13*, 429; R. Papoular, A. Zheludev, E. Ressouche, J. Schweizer, *Acta Crystallogr. Sect. A*, **1995**, *51,* 295.
[30] S. F. Gull, J. Skilling, *MEMSYS Users Manual*, **1989**, Maximum Entropy Data Consultants Ltd, 33 North End, Meldreth, Royston SG8 6NR (England).
[31] A. Zheludev, R. Papoular, E. Ressouche, J. Schweizer, *Acta. Crystallogr. Sect. A* **1995**, *51*, 450.
[32] J. Skilling, "The Axioms of Maximum Entropy" in *Maximum Entropy and Bayesian Methods in Science and Engineering*, *Vol. 1* (Eds.: G. J. Erickson, C. R. Smith), Kluwer, **1988**, 173.
[33] C. Moller, M. S. Plesset, *Phys. Rev.* **1934**, *46*, 618.
[34] I. Shavitt, "Methods of Configurational Interaction" in *Modern Theoritical Chemistry*, *Vol. 3*(Ed.: H. F. Shaefer, III), Plenum, New York, **1977**, 189.
[35] W. Kohn, L. J. Sham, *Phys. Rev. A*, **1965**, *11*, 1133.
[36] DGAUSS UniChem4, Cray Research Inc., Cray Research Park, 655 Lone Oak Drive, Eagan, MN 55121.
[37] S. H. Vosko, L. Wilk, M. Nausair, *Can. J. Phys.* **1980**, *58*, 1200.
[38] J. P. Perdew, *Phys. Rev. B* **1986**, *33*, 8822.
[39] A. D. Becke, *Phys. Rev. A* **1988**, *38*, 3098.
[40] J. Goldman, T. E. Petersen, K. Torssell, *Tetrahedron* **1973**, *29*, 3833.
[41] H. M. McConnell, *J. Chem. Phys.* **1963**, *39*, 1910.
[42] H. M. McConnell, *Proc. Robert A. Welch Found. Conf. Chem. Res.* **1967**, *11*, 144.

Received: January 28, 1999
Revised version: May 17, 1999 [F1573]

  0947-6539/99/0512-3624 $ 17.50+.50/0